

Identification, enhancement and time-resolved study of YIG spin wave modes in a MW cavity in strong coupling regime

Angelo Leo^a, Silvia Rizzato^b, Anna Grazia Monteduro^{a,b}, Giuseppe Maruccio^{a,b}

^a Mathematics and Physics Department “E. De Giorgi”, University of Salento, Lecce, Italy

^b INFN-Sezione di Lecce, Lecce, Italy



Spintronics Lab



- Cryogenic superconducting magnet (10.5 T, 0.3-300 K)
- Oxford dilution refrigerator (down to 10 mK, vector magnet 6T/1T/1T)
- Cryogenic RF probe station (down to 8 K and up to 0.5 T and 70 GHz).



Italian node of the European Infrastructure on Magnetism (funded within ISABEL project, H2020-INFRADEV-2018-2020, Grant No. 871106).



Magnonics

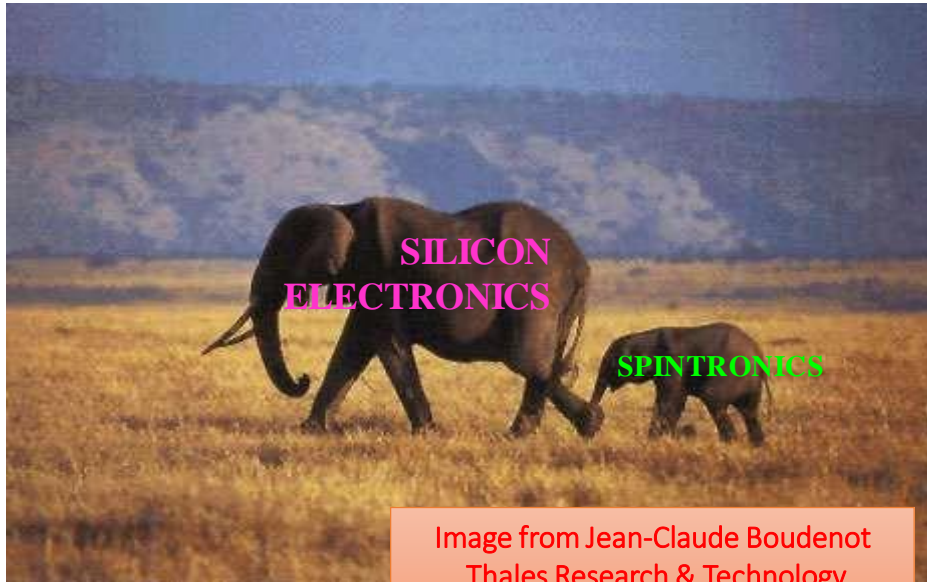
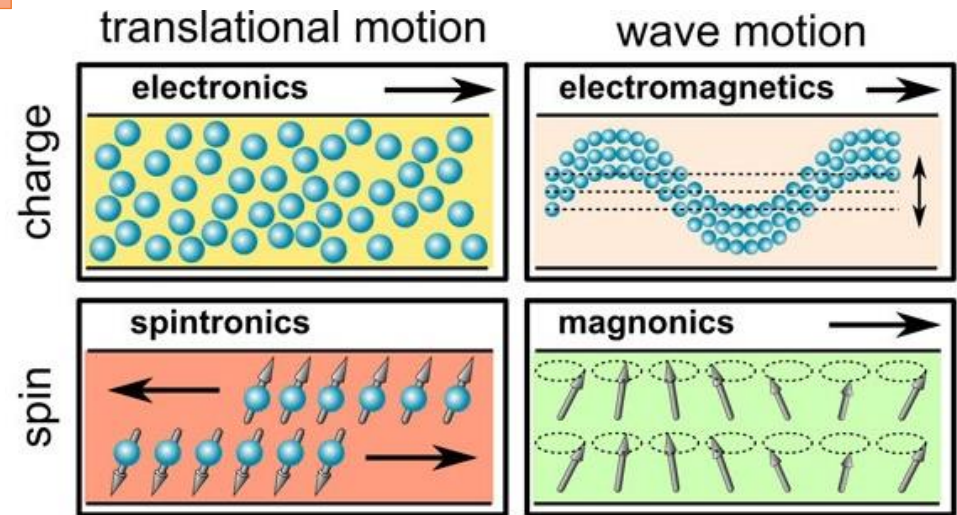
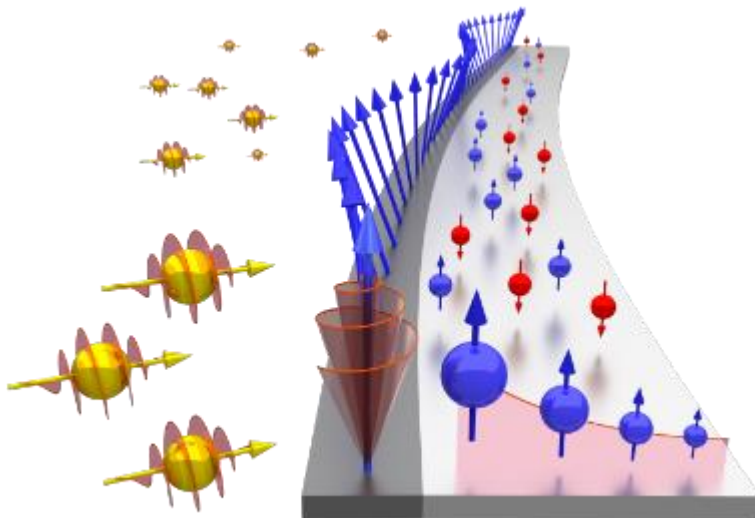
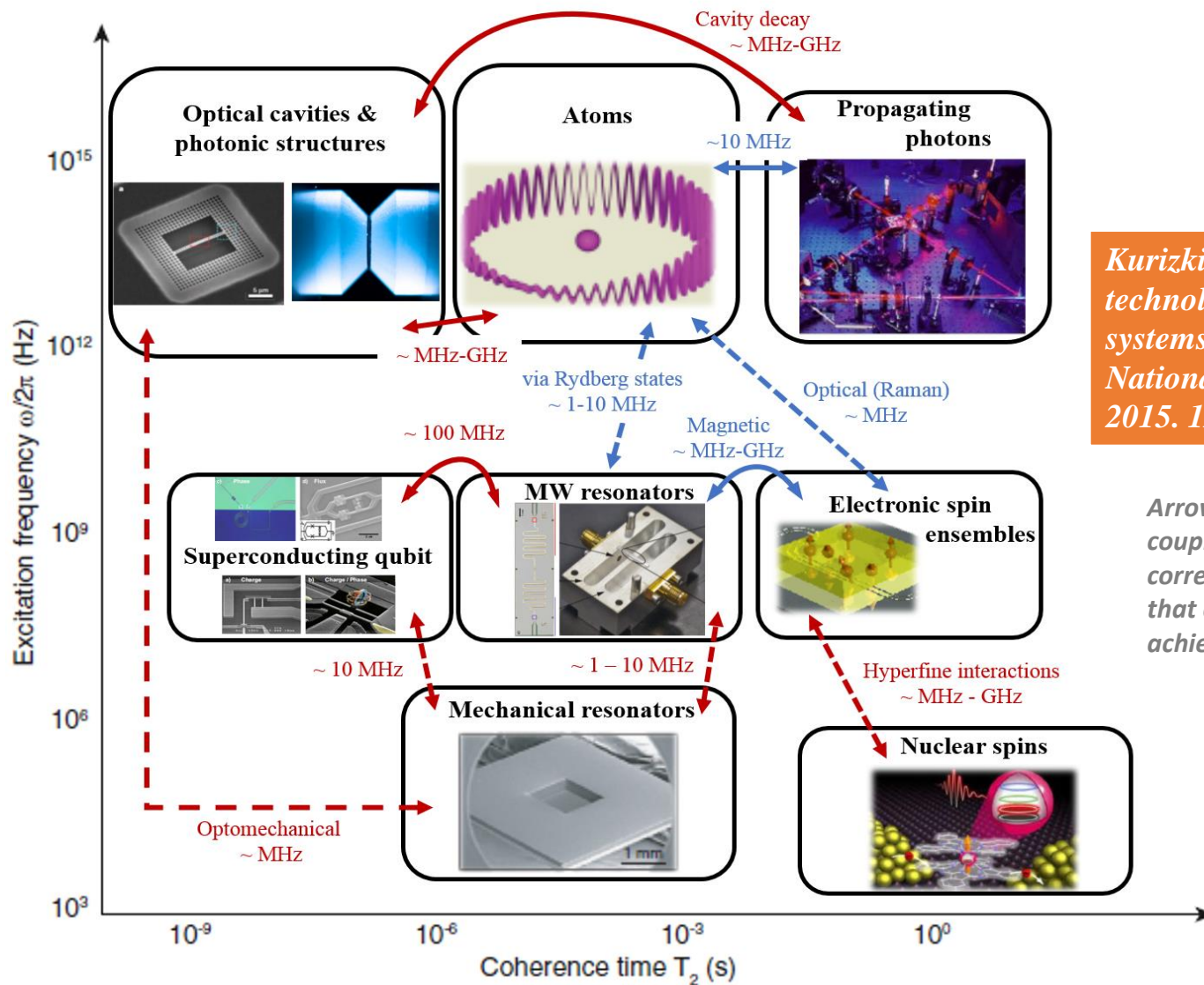


Image from Jean-Claude Boudenot
Thales Research & Technology



Towards quantum technologies with hybrid systems

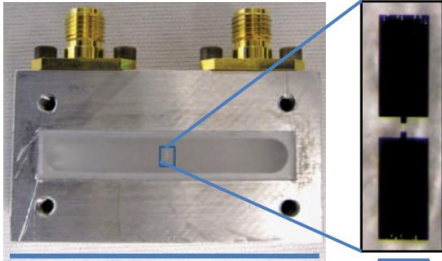


Kurizki, G., et al., Quantum technologies with hybrid systems. Proceedings of the National Academy of Sciences, 2015. 112(13): p. 3866-3873.

Arrows indicate possible coupling mechanisms and the corresponding coupling strength that can be realistically achieved.

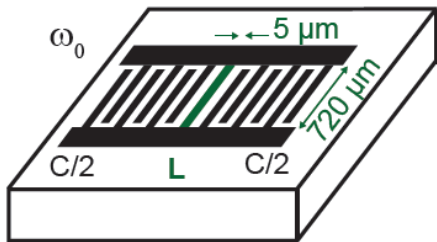
Cavity QED and hybrid systems for QC

SC / TRASMON

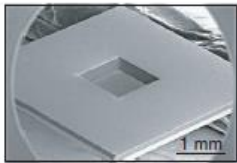


Paik et al, Phys Rev Lett (2011)

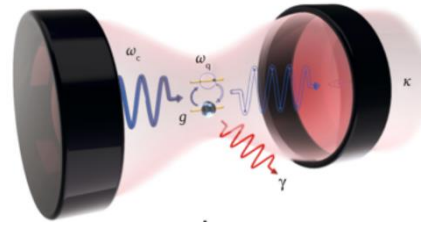
OMR / PHONONS



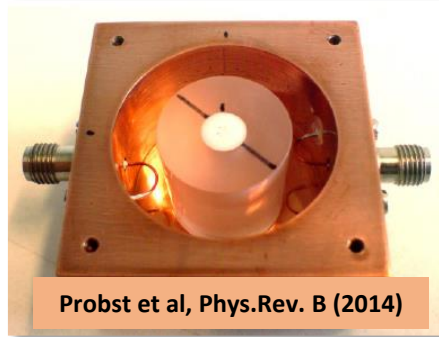
Bienfait et al, Nature Lett. (2016)



Yuan et al, Nature Comm. (2015)



3D MW Cavities



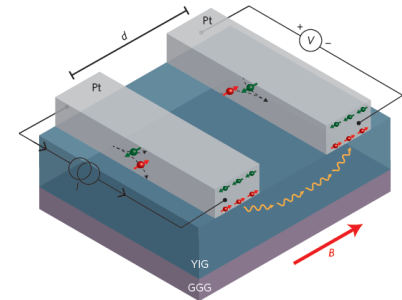
Probst et al, Phys.Rev. B (2014)

PARAMAGN. SPIN ENSEMBLES

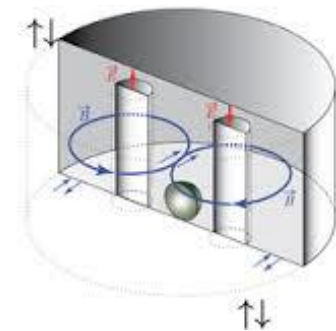


Putz et al, Nature Physics (2014)

FM MATERIALS



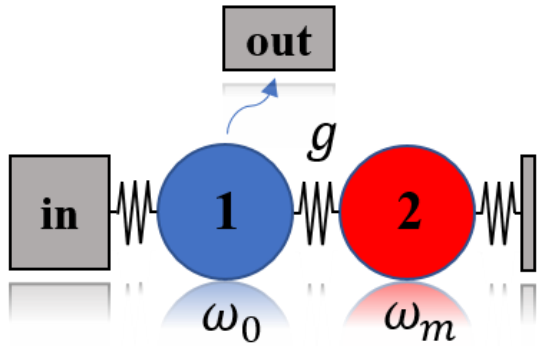
Cornelissen et al, Nature Physics (2015)



Goryachev et al, Phys Rev App (2014)



Magnon-Photon coupling



Confined EM field

$$\mathcal{H}_c = \hbar\omega_0 \left(a^\dagger a + \frac{1}{2} \right)$$

Magnons

$$\mathcal{H}_m = \hbar\omega_m \left(m^\dagger m + \frac{1}{2} \right)$$

only with resonant interactions:

$$\mathcal{H} = \mathcal{H}_c + \mathcal{H}_m + \mathcal{H}_{int} \quad \frac{\mathcal{H}}{\hbar} = \omega_0 a^\dagger a + \omega_m m^\dagger m + \underline{g} (a^\dagger m + m^\dagger a)$$

Coupling strength of each spin:

$$\frac{g_{0,i}}{2\pi} = \frac{\left(\eta \gamma_e \sqrt{\frac{(\mu_0 \hbar \omega_0)}{V_c}} \right)}{4\pi}$$

As a spin ensemble:

$$g_i = g_{0,i} \sqrt{N_s}$$

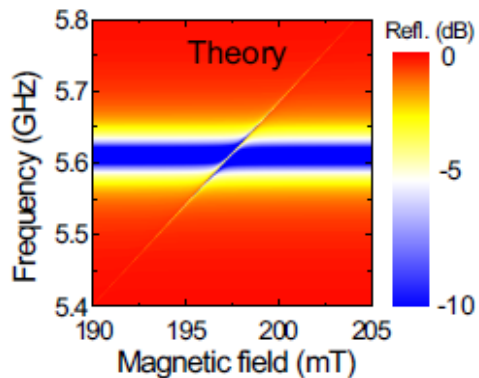
$$g_i \propto \sqrt{\omega_{eff}} = \sqrt{\omega_0 V_m / V_a}$$

Overlap among subsystems:

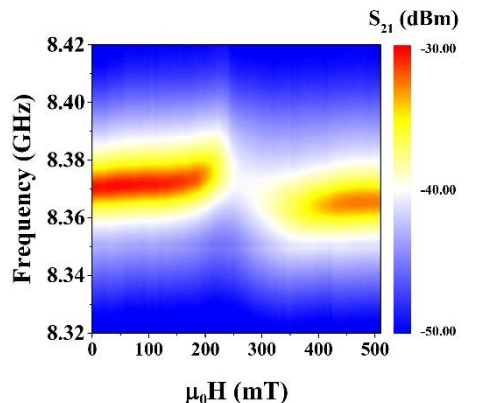
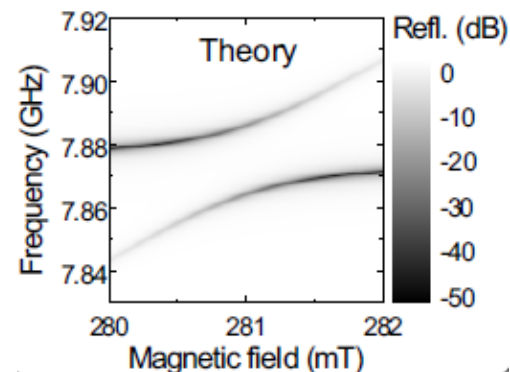
$$\eta = \int_{V_m}^0 \frac{\vec{h} \cdot \vec{M}}{|\vec{h}_{max}| |\vec{M}_{max}|} dV \leq 1$$

Magnon-Photon Coupling Regimes

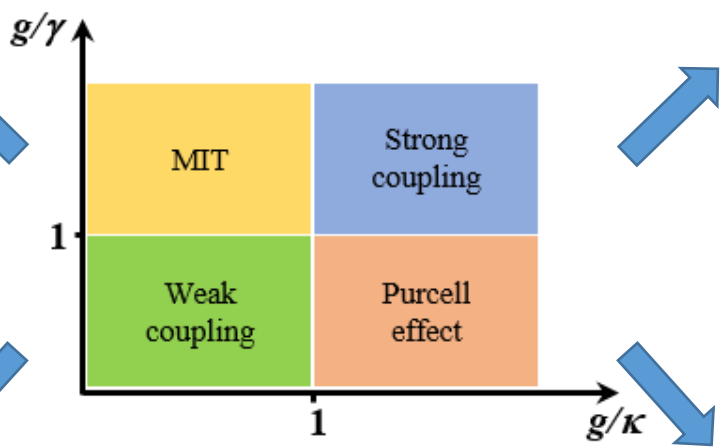
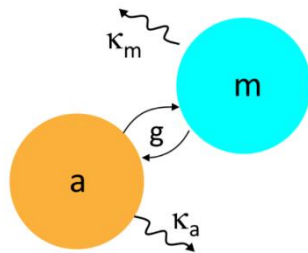
Zhang et al, Phys Rev Lett (2014)



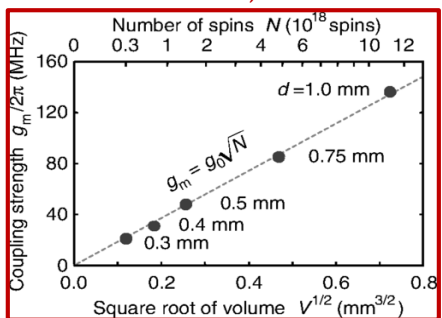
Zhang et al, Phys Rev Lett (2014)



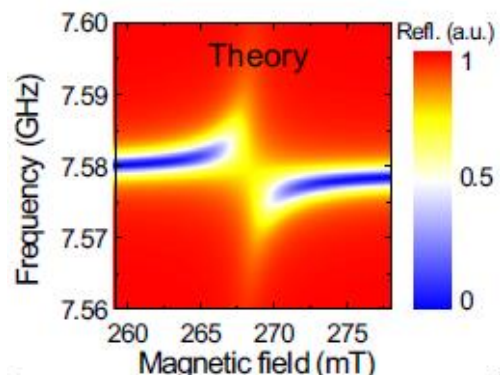
Mn_2FeO_4 NPs in a low Q cavity (Unisalento)



$$g_i = g_{0,i} \sqrt{N_s}$$



Y. Tabuchi et al. PRL (2014)

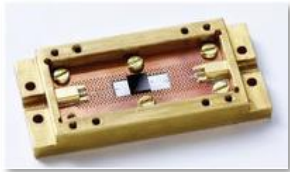


Zhang et al, Phys Rev Lett (2014)

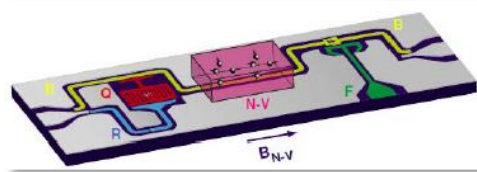
Increasing coupling via spin density (& YIG)

Paramagnetic spin ensembles

NV- centers in diamond

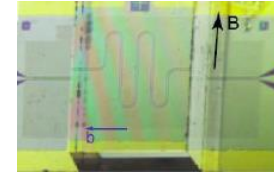


Putz et al., *Nature Physics* 10, 720–724 (2014)



Kubo et al. *PRL* 107, 220501 (2011)

Rare-earth doped crystal



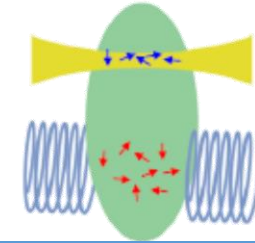
Bushev et al. *PRB* 84, 060501(R) (2011)

Low spin density: 10^{12} - 10^{18} cm⁻³

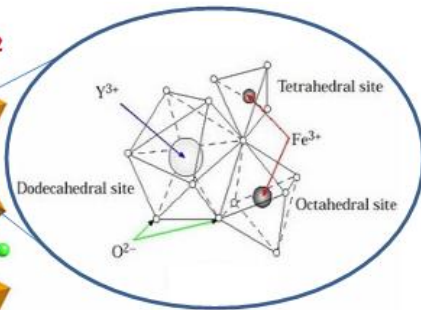
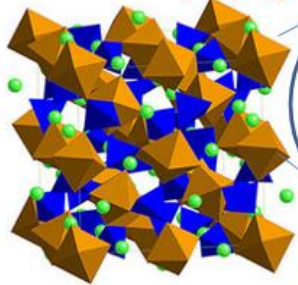


Optical Light

Microwave



YIG = $Y_3Fe_5O_{12}$



High net spin density 2.1×10^{22} cm⁻³



& very low damping

Microwave oscillator



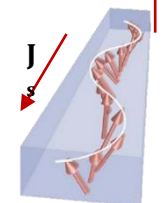
CANDOX Corp.

Optical isolator



FDK Corp.

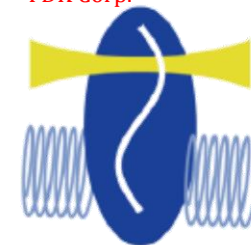
Spintronics/
Magnonics



Kajiwara et al.
doi:10.1038/nature08876

Optical Light

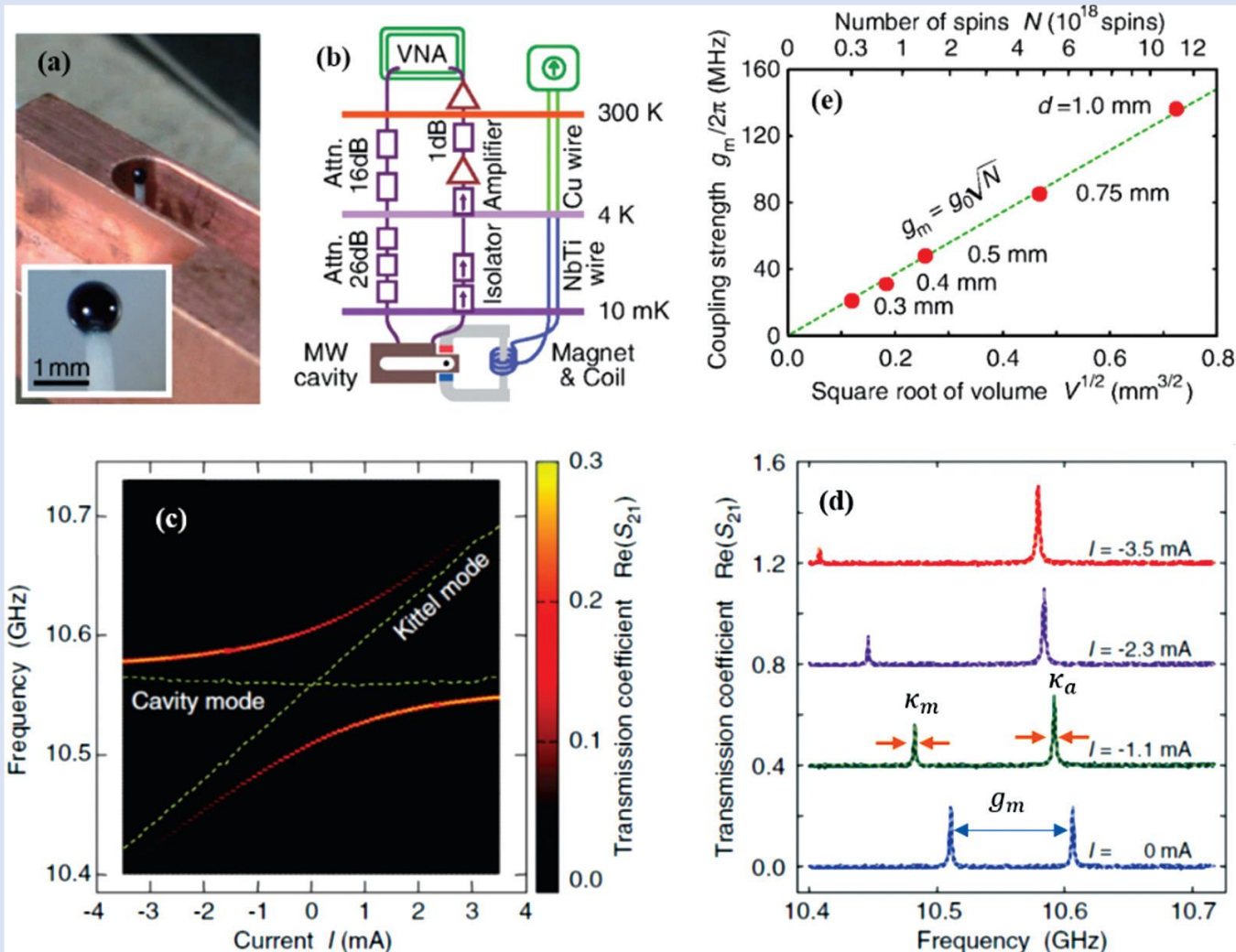
Microwave



**Strong
Coupling**



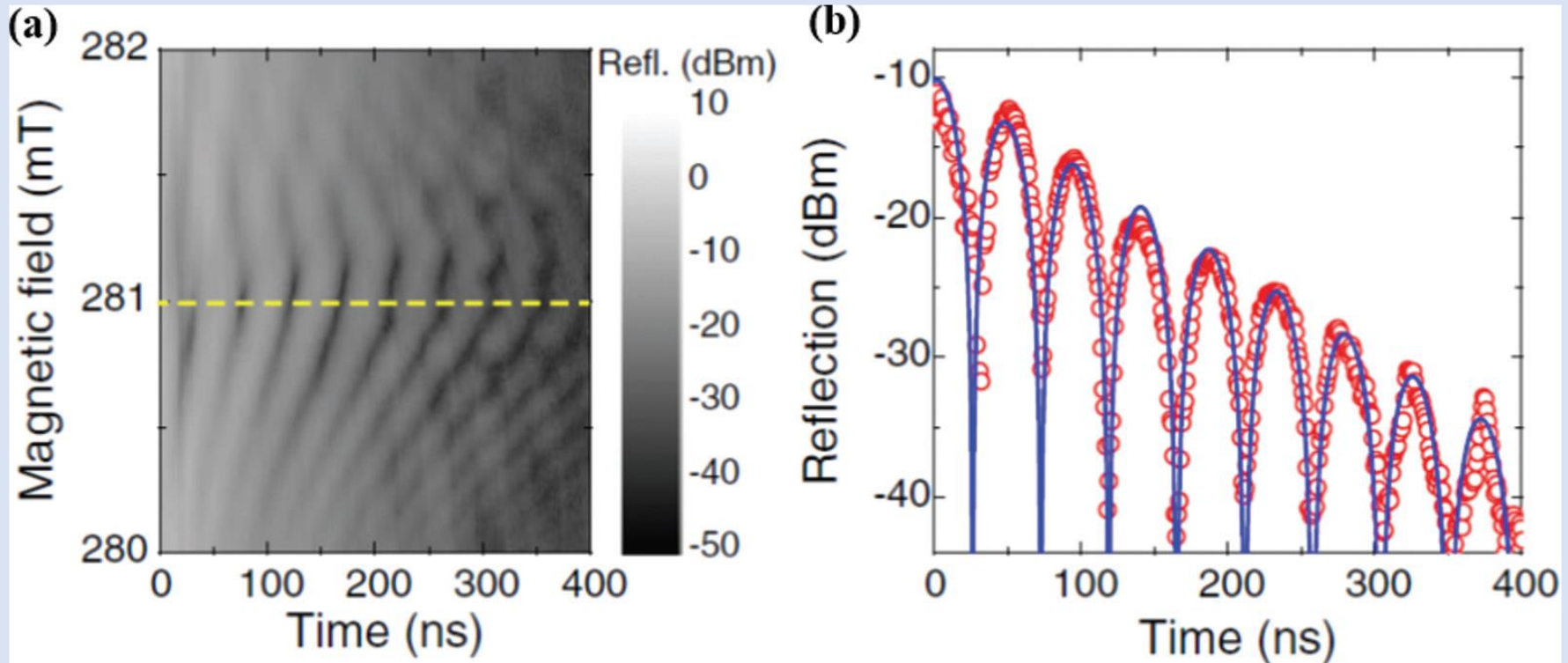
Strong Coupling & exp. setup



Y. Tabuchi, S. Ishino, T. Ishikawa, R. Yamazaki, K. Usami and Y. Nakamura (2014). Hybridizing ferromagnetic magnons and microwave photons in the quantum limit, *Physical review letters*, **113**(8): 083603.



Rabi-like oscillations



(a) Evolution of the cavity response after a pulsed signal modulated at cavity's eigenfrequency as a function of bias magnetic field. (b) Measured Rabi-like oscillation signal at bias magnetic field such that YIG FMR occurs.

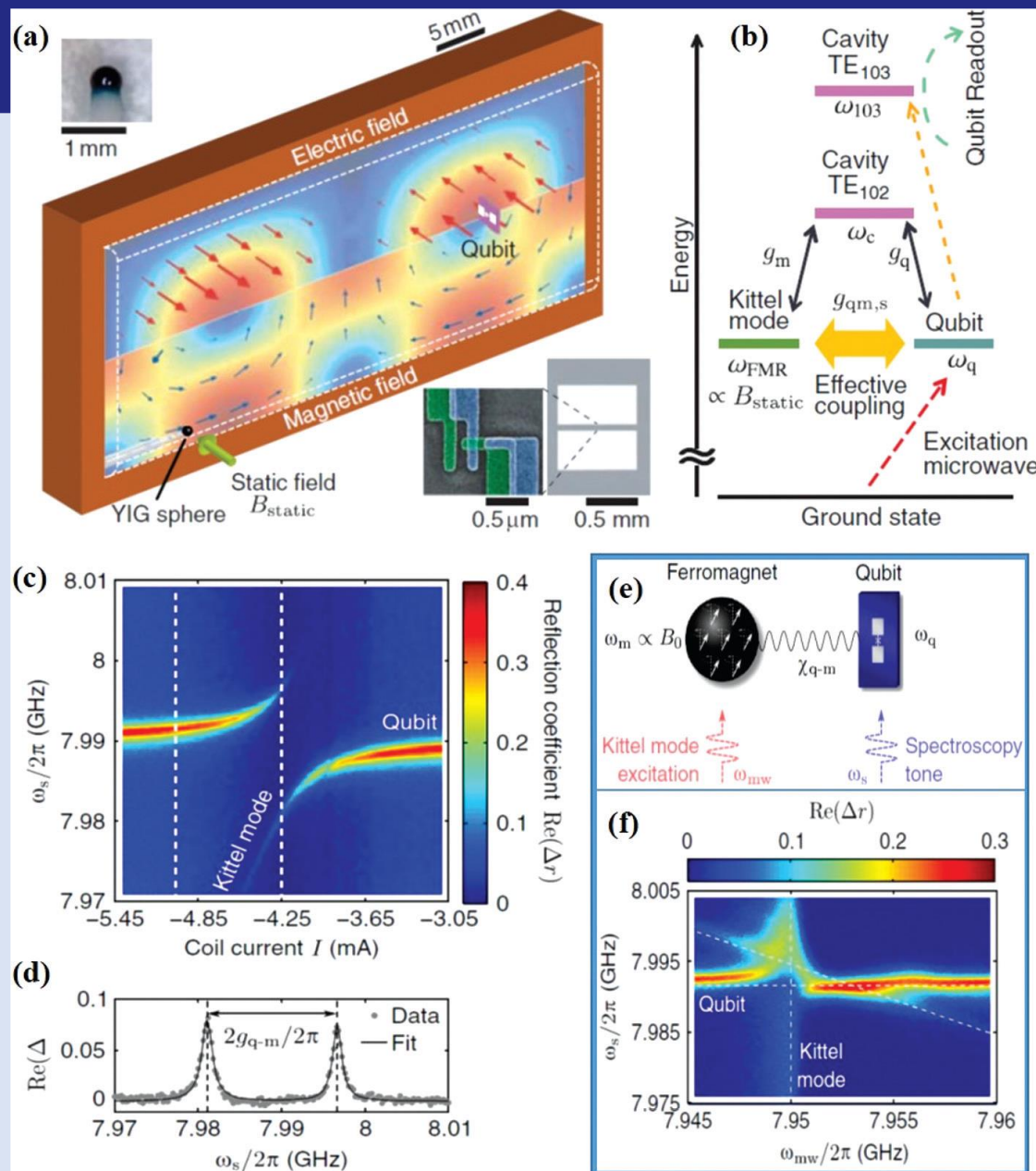
X. Zhang, C.-L. Zou, L. Jiang and H. X. Tang (2014). Strongly coupled magnons and cavity microwave photons, *Physical review letters*, 113(15): 156401.

Coupling with trasmons

hybrid system in the strong dispersive regime, composed by an FM crystal, a superconducting transmon, and a 3D MW cavity

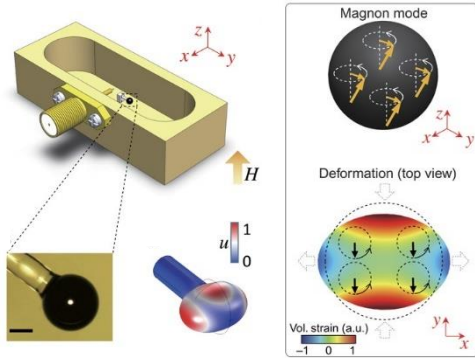
Y. Tabuchi, S. Ishino, A. Noguchi, T. Ishikawa, R. Yamazaki, K. Usami and Y. Nakamura (2015). Coherent coupling between a ferromagnetic magnon and a superconducting qubit, *Science*, 349(6246): 405–408.

D. Lachance-Quirion, Y. Tabuchi, S. Ishino, A. Noguchi, T. Ishikawa, R. Yamazaki and Y. Nakamura (2017). Resolving quanta of collective spin excitations in a millimeter-sized ferromagnet, *Science advances*, 3(7): e1603150.



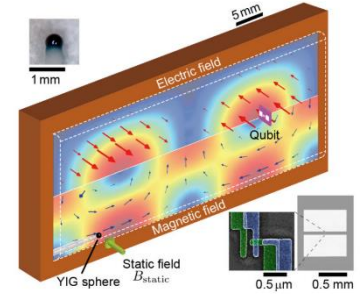
Cavity Magnonics with YIG

Phononic coupling with magnons



X. Zhang et al, Science Advances (2016)

Coupling with transmon

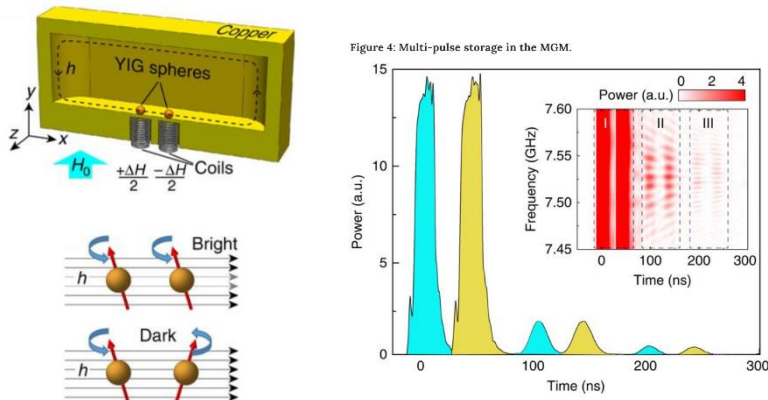


Tabuchi et al, Science (2015)

Room temperature

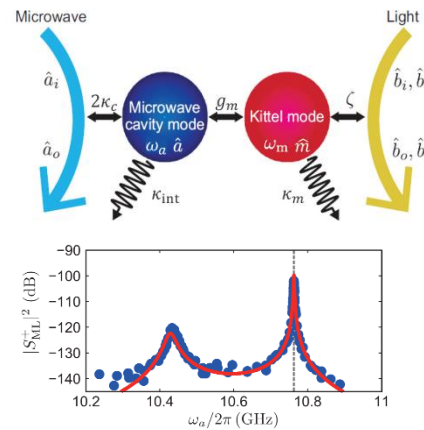
Low temperature

Magnon dark modes and gradient memories



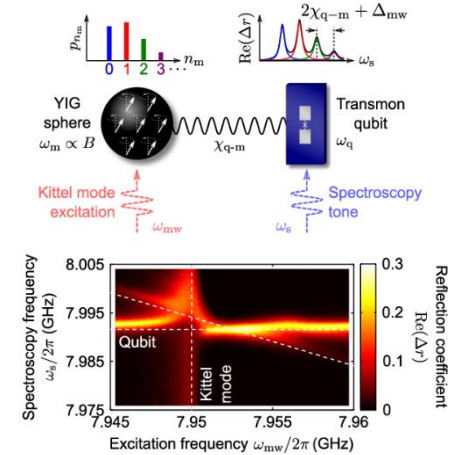
X. Zhang et al, Nature Comms (2015)

MW – opt. conversion



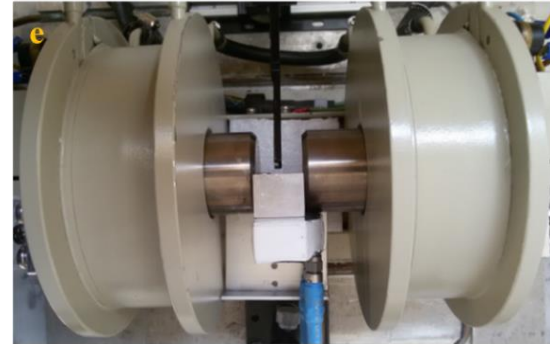
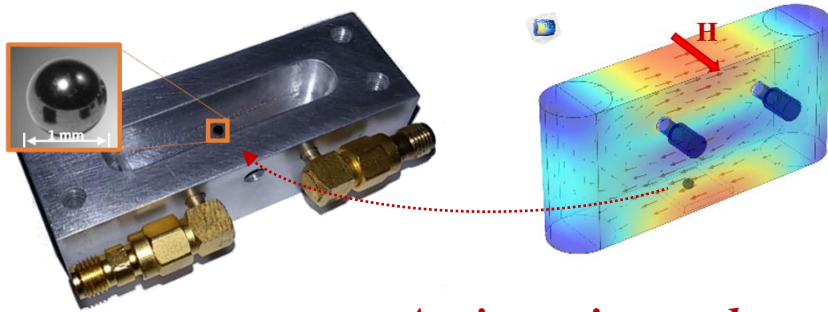
Hisatomi et al, Phys. Rev B (2016)

Resolving magnon number



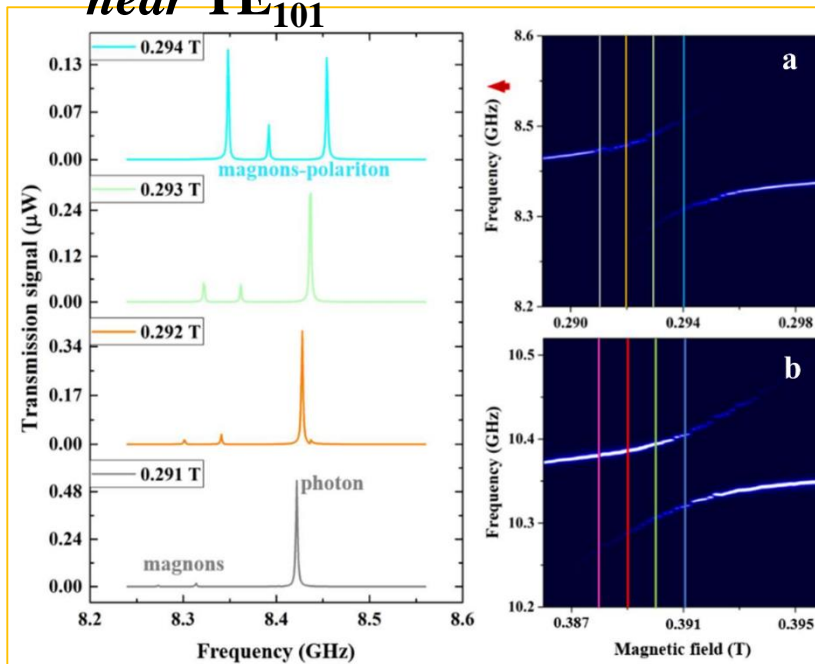
Lalanche-Quirion et al, Science Advances (2017)

Strong coupling fingerprints (1/2)

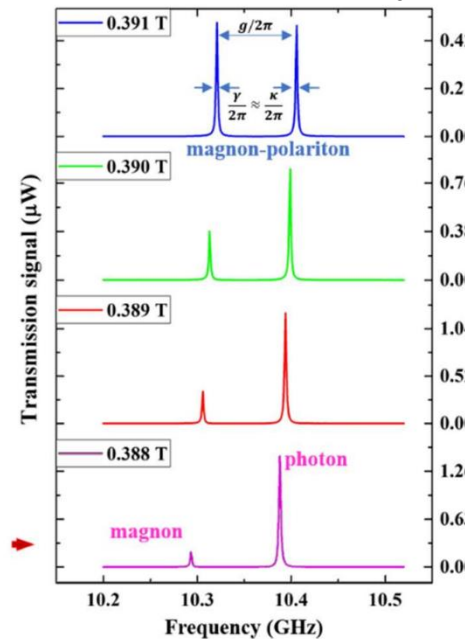


Anticrossing and magnon-polaritons

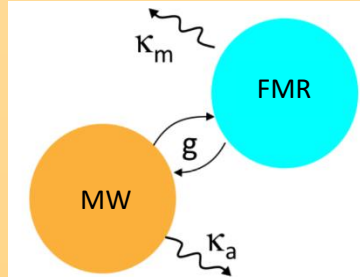
near TE_{101}



near TE_{102}



Magnon mode damping rate:
 κ_m ($m = \text{FMR, MSMs}$)
 Magnon mode at
 ω_m ($m = \text{FMR, MSMs}$)

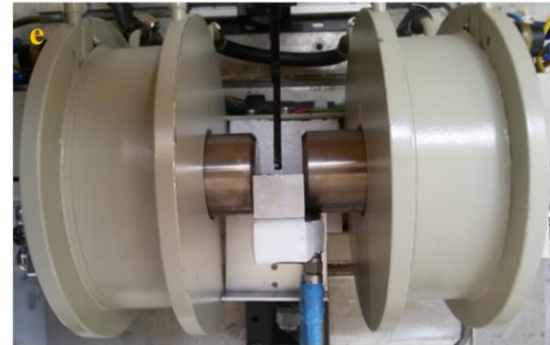
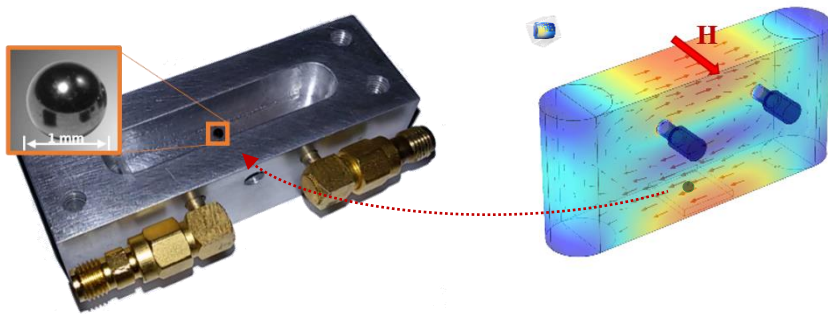


Cavity mode at:
 ω_c
 Total cavity decay rate:
 $\kappa_c = \frac{1}{2}(2\kappa_{i,o} + \kappa_{int})$

Coupling strength
 g_m ($m = \text{FMR, MSMs}$)

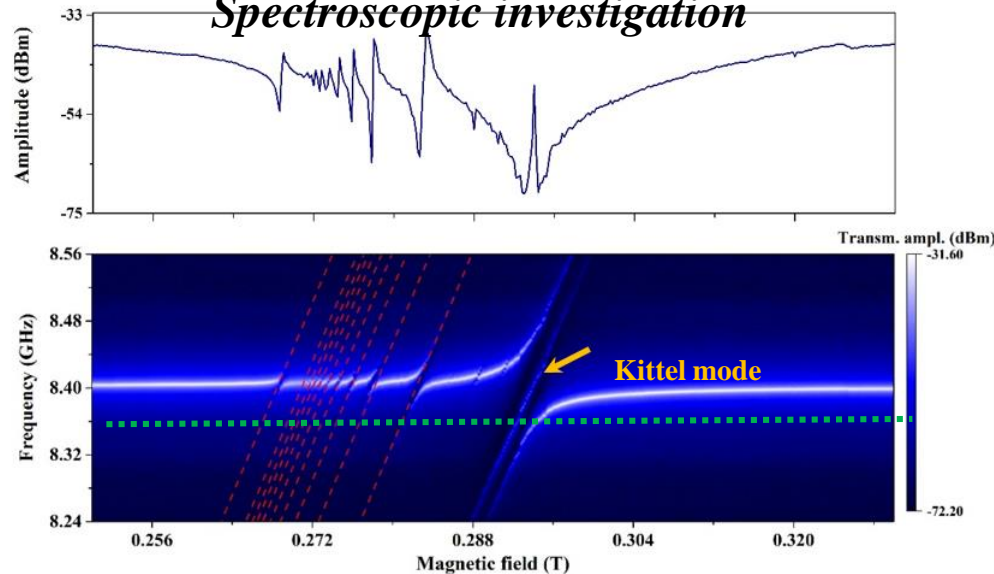
Strong coupling between fundamental mode in the YIG sphere and the TE_{101} and TE_{102} cavity modes.

Strong coupling fingerprints and MSMs



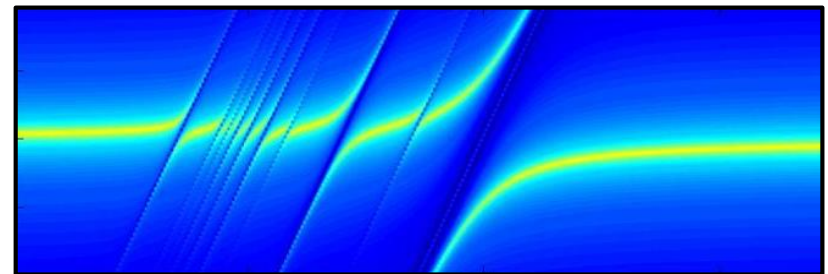
Rich spectrum with MSMs

Spectroscopic investigation



input-output formalism

$$T(\omega) = \frac{\kappa_c}{i(\omega - \omega_c) - \kappa_c + \sum_m \frac{|g_m|^2}{-\frac{1}{2}\kappa_m + i(\omega - \omega_m)}}$$



Magnetostatic modes of a sphere

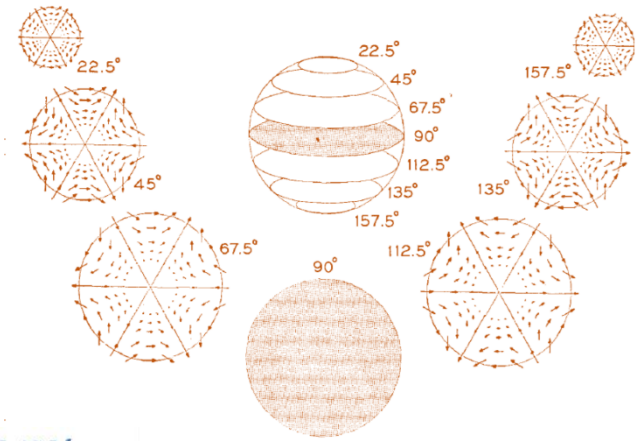


Characteristic equation in associated Legendre functions P_n^m for **MSMs in spheroids** within MW cavity working at frequency $f = \omega_c/2\pi$

$$n + 1 + \xi_0 \frac{P_n^{m'}(f, H_0)}{P_n^m(f, H_0)} \pm m \frac{\gamma f M_S}{\gamma^2 H_i^2 - f^2} = 0$$

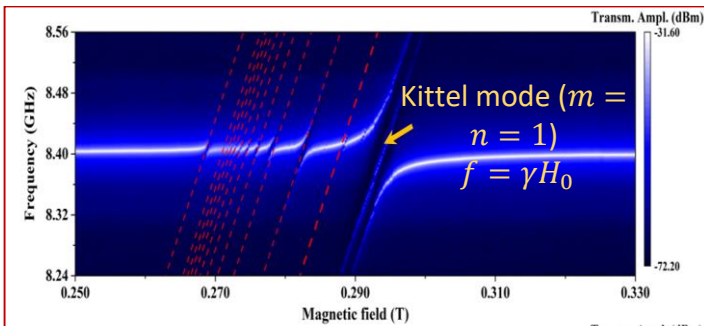
$$\frac{f}{\gamma M_S} - \frac{H_{0,mm}}{M_S} + \frac{1}{3} = \frac{m}{2m+1} \quad (n = m)$$

$$\frac{f}{\gamma M_S} - \frac{H_{0,m(m+1)}}{M_S} + \frac{1}{3} = \frac{m}{2m+3} \quad (n = m + 1)$$

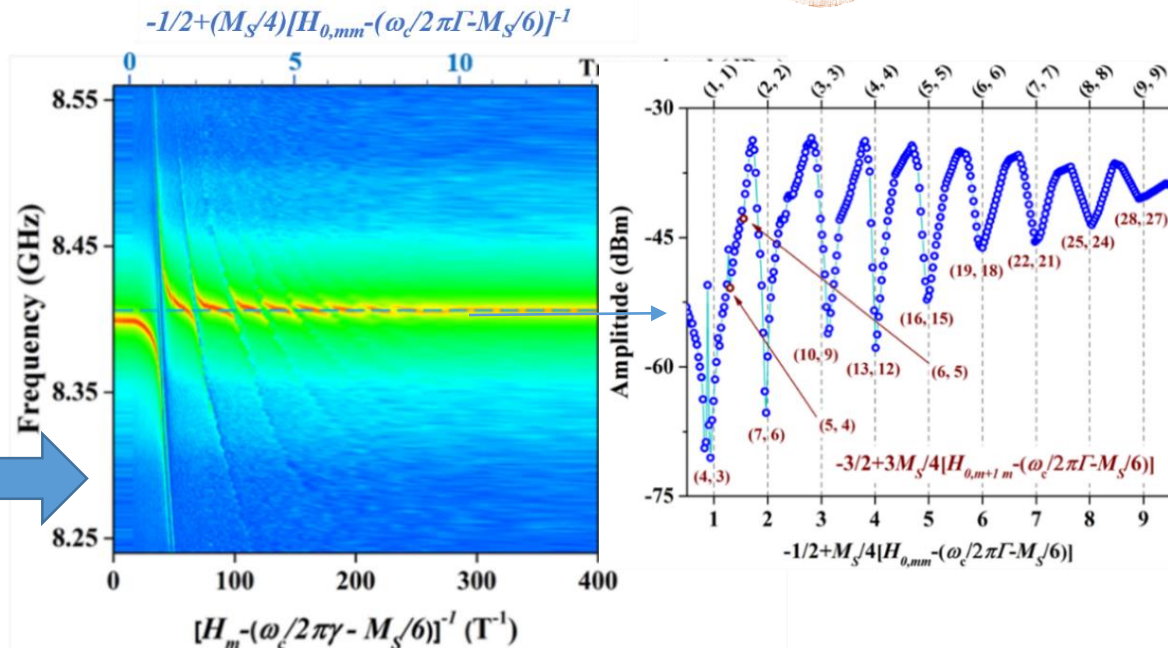


Proposed strategy:

introduce functional plot variable:



rescaled by using: $\gamma \approx 28.76 \text{ GHz/T}$
 $M_S \approx 0.176 \text{ T}$

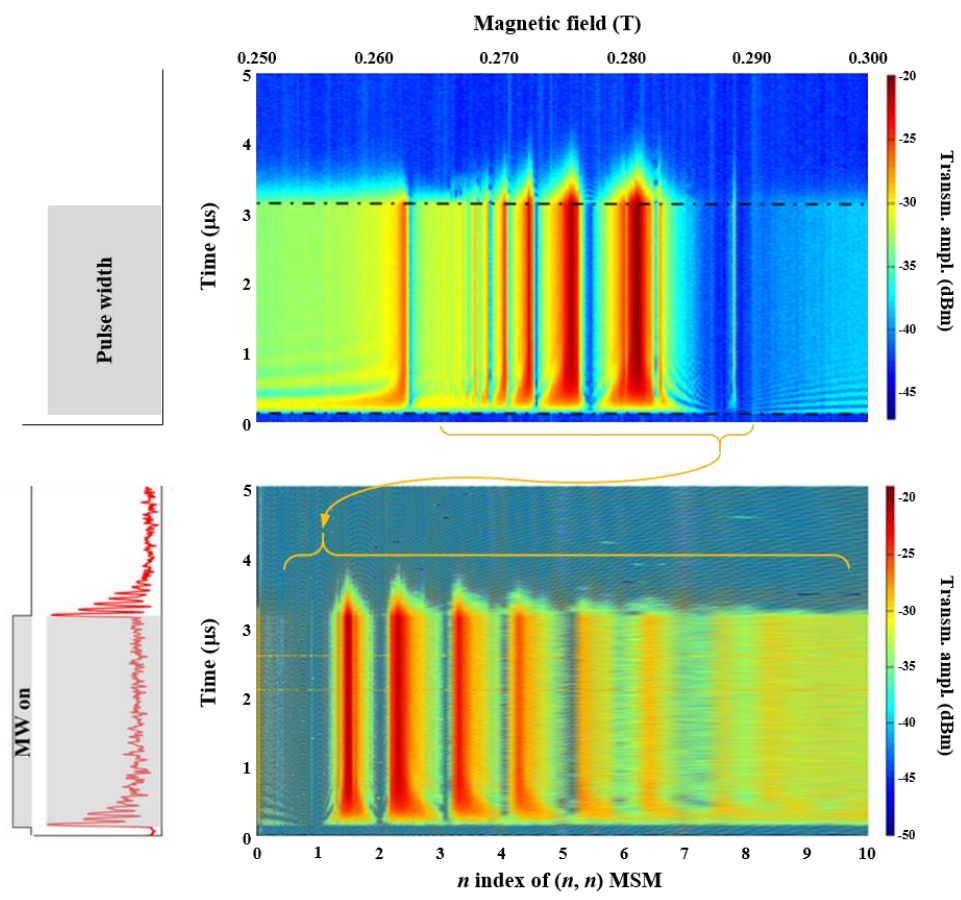


Strong coupling fingerprints (2/2)

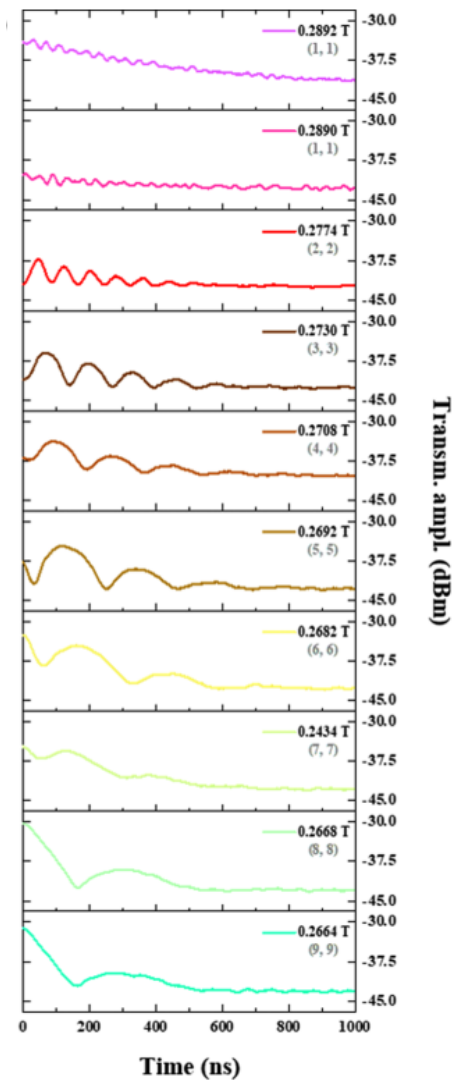
$$P\left(\frac{\omega_i}{2\pi}\right) \propto A_i \cdot \log \left[\sin^2\left(\frac{g_i}{2\pi} t\right) \cdot \exp\left(-\frac{2\kappa_c - \kappa_{int}}{2\pi} t\right) \right]$$



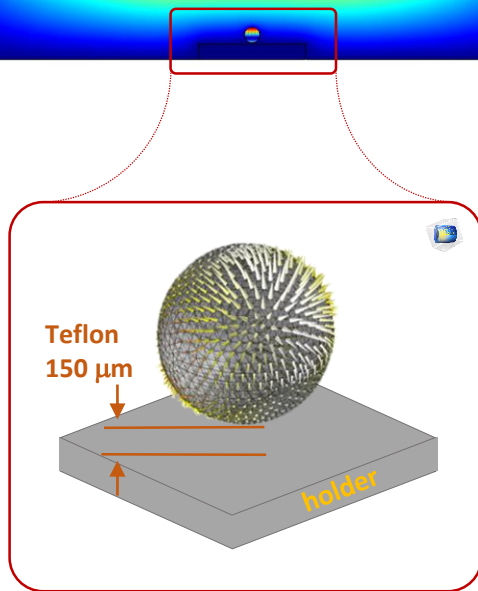
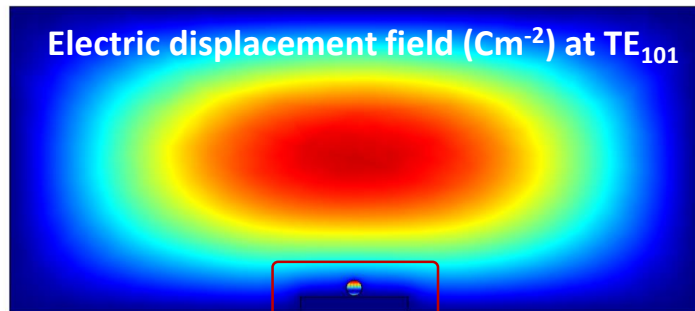
Coupling among resonators MW cavity relaxation



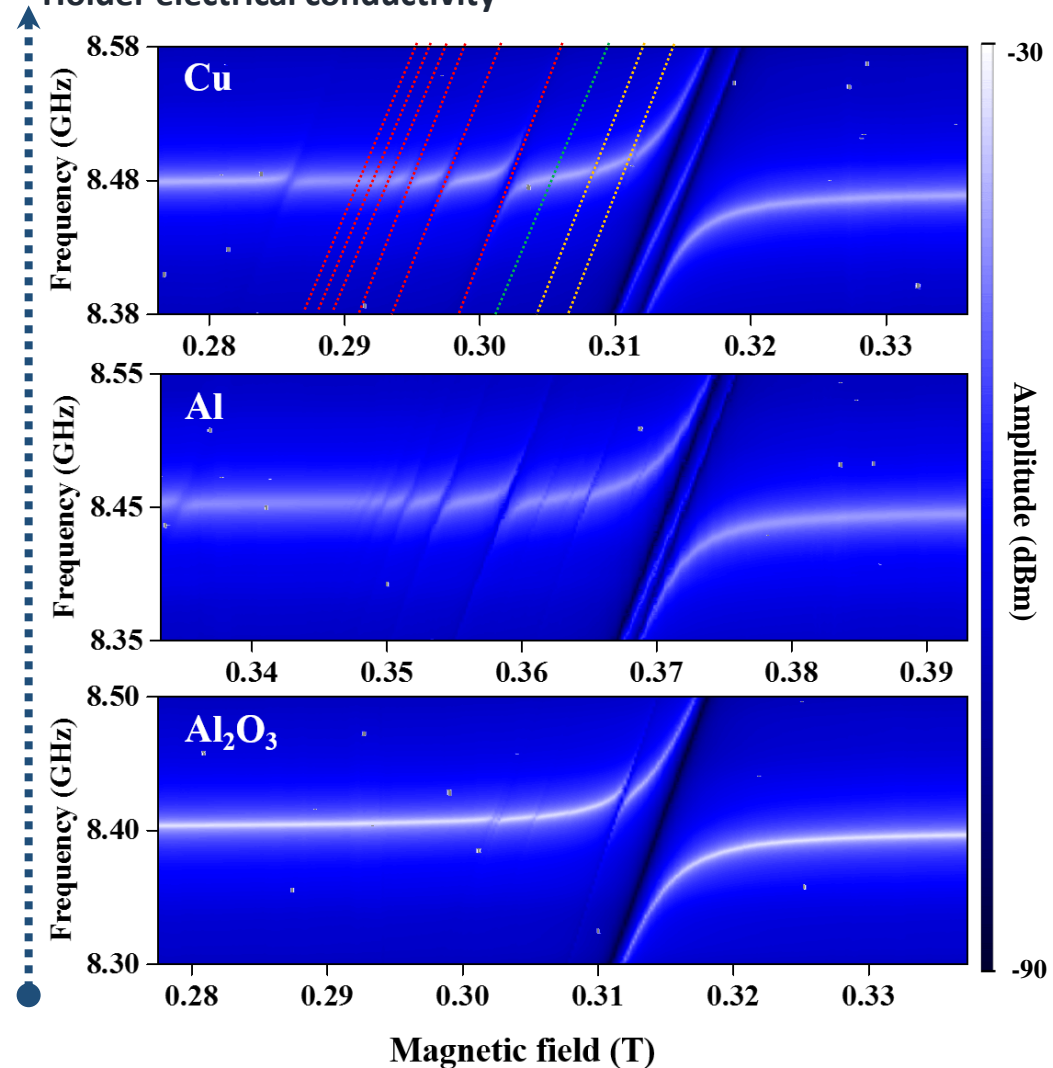
Cavity relaxation @ CMP formation



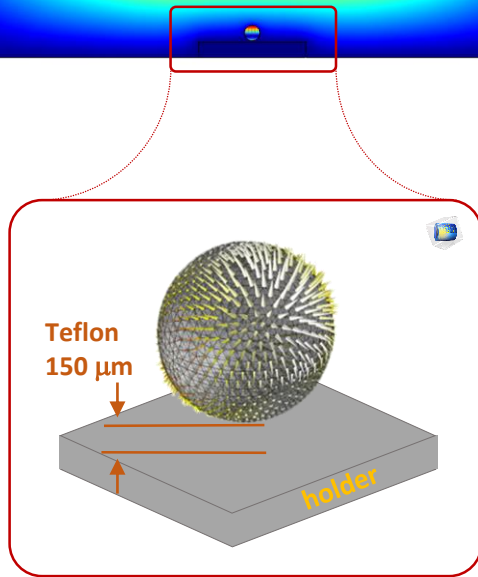
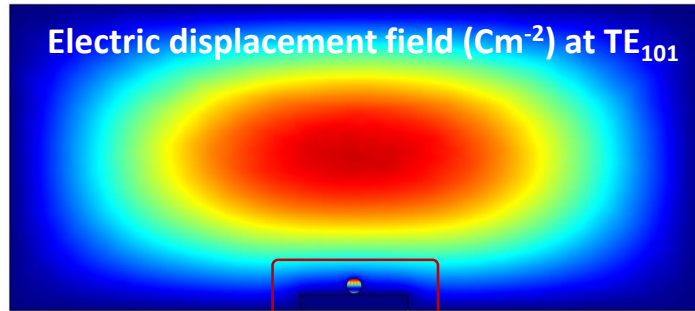
Enhancement of coupling features



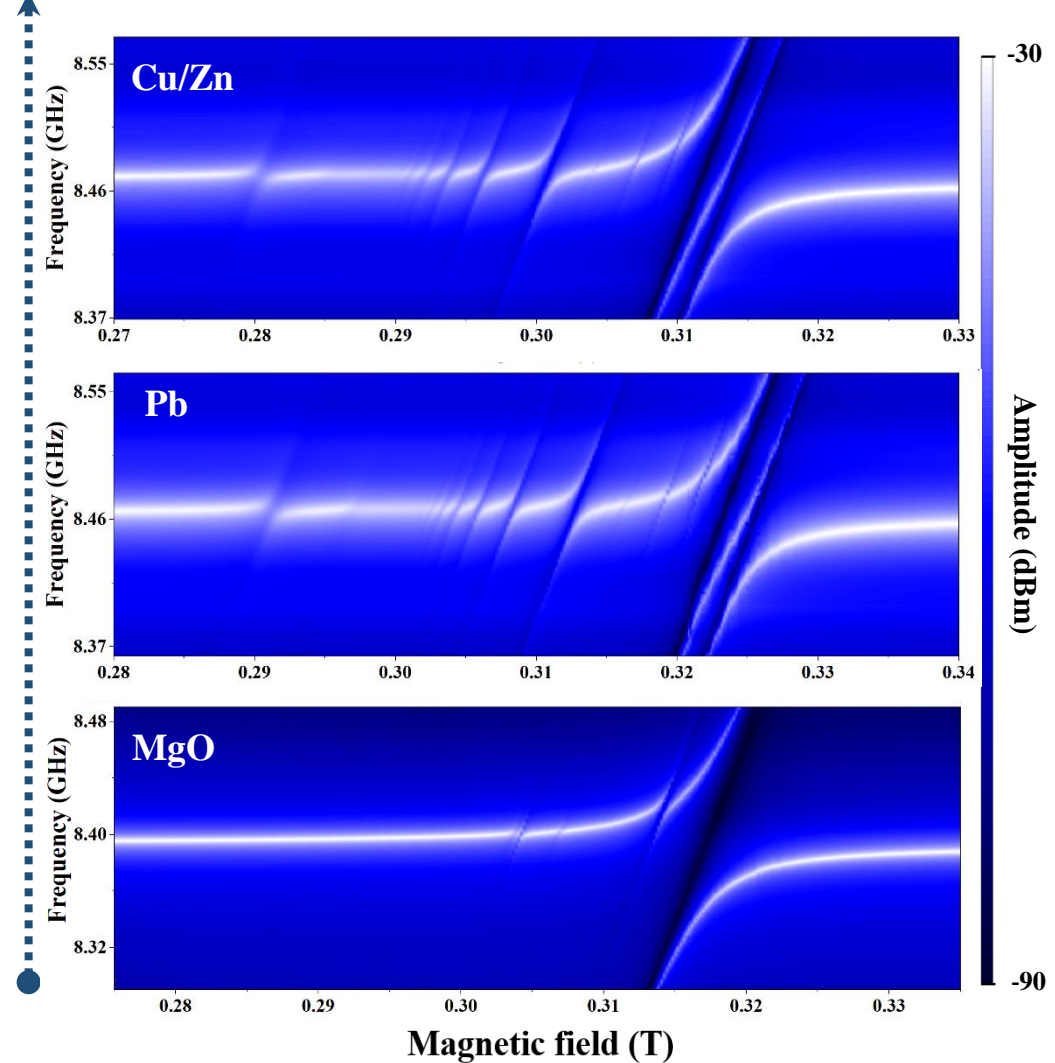
Holder electrical conductivity



Enhancement of coupling features



Holder electrical conductivity



Enhancement of coupling features

